Principal component analysis and Steerable Pyramid Transform Image Denoising Method for Gray Scale

Prachi Tiwari, Ayoush Johari, Dr. Soni Changlani

Abstract— **This paper suggests a spatially adaptive image denoising scheme, which is comprised of two stages. In the first stage, image is denoised by using Principal Component Analysis (PCA) with Local Pixel Grouping (LPG). LPG-PCA can effectively preserve the image fine structures while denoising. In the second stage, we use Steerable Pyramid Transform (SPT) to decompose images into frequency sub-bands. The noise level is updated adaptively before second stage denoising. Steerable Pyramid Transform in the second stage further improves the denoising performance. This paper also reviews on the present denoising processes and performs their comparative study. Experimental results demonstrate that the proposed PCA-SPT algorithm achieve competitive outcomes. PCA-SPT works well in image fine structure preservation, compared with state-of-the-art denoising algorithms.**

Index Terms— **AWGN, Wavelet, SPT, LPG-PCA, BM3D, Edge preservation.**

I. INTRODUCTION

Digital image processing is a discipline that goes forward, to grow, with new application being developed at an invariably enhancing stride. It is a fascinating and stimulating field to be involved in today with application areas ranging from the entertainment industry to the space program. In the 21^{st} century, a digital image is the best possible substitute to convey visual information from one place to another. Digital image processing is a specific class of signal processing, whose primary objective is to extract the essential information from the contaminated images. Ideally, this is achieved with the help of computers, by applying some best available algorithms. As the essential information is extracted from the contaminated images the next step is to apply standard techniques to it, which will remove the artifacts presents in the contaminated image.

Image denoising shares an eminent portion of digital image processing, which is an essential step to remove the artifacts and improve the tone of the images. It is a prerequisite for many image processing tasks like image classification, image registration, image restoration, image segmentation and object recognition, where it is essential to suppress the artifacts from the noisy image to get the approximately original image. Noise will be brought into an image through the image acquisition process such as quantization, transmission due to a noisy channel and errors from the measurement process. Each step of the image acquisition process successively degrades image such as lenses, film, digitizer, etc. contribute to the degradation procedure.

Image denoising is an obligatory procedure in real world applications such as photography where an image was necessarily degraded but needs to be improved before it can be published. For this type of application, we have to develop a model [1], which better describes the degradation process. This model helps to determine the inverse process, which can be applied to the image to get it back into the original form. Space exploration is one such example in which image restoration is frequently used to eradicate artifacts, generated by mechanical movement of the space vehicle or to reduce distortion in the optical system of a telescope. Astronomy is another important application, where we generally deal with the images of poor resolution. Image processing plays an important role in the medical science imaging system also, where quality processing techniques are required for probing images of unparalleled events and in forensic science, to enhance the quality of potentially useful photographic evidence of extremely bad quality.

Noise will be necessarily brought into the image acquisition process, hence for further execution, denoising is an essential step to improve the quality of the image. Since image denoising is an introductory step thus it has been extensively studied and many denoising algorithms have been suggested, from the initially developed filters and transform domain noise removal techniques to the recently invented wavelet [5] transform, curvelet [28] and ridgelet [29] based methods, sparse representation [4] and K-SVD [7] methods, shape-adaptive transform [3], bilateral filtering [9], non-local mean based denoising [10,11] and non-local collaborative filtering [12]. With their increasingly broad applications in our everyday life and the rapid growth of modern digital imaging devices, there are increasing demands of new denoising techniques to obtain higher quality of image.

There are various denoising algorithms [5] based on Wavelet Transform (WT) [13] gives better results than comparative techniques. In WT the input signal is decomposed into multiple scales. Each scale symbolizes different time-frequency constituents of the original signal. In wavelet transform, for the removal of noise it is necessary to perform certain processes, such as thresholding [1] and statistical modeling [2]. Denoising is achieved by transforming back the processed wavelet coefficients into time domain. Recent development of WT denoising includes curvelet [4] and ridgelet [5] methods for the preservation of line structure.

Manuscript received Dec, 2015.
***Prachi Tiwari**, Department of Electronics and Communiction, LNCTS Bhopal, Bhopal, India , 9826736156*
***Ayoush Johari**, Department of Electronics and Communiction, LNCTS Bhopal, Bhopal, India*
***Dr. Soni Changlani**, Department of Electronics and Communiction, LNCTS Bhopal, Bhopal, India ,*

ISSN: 2278 – 7798

WT-based denoising algorithms may introduce many visual artifacts in the output image, since WT-based denoising uses fixed wavelet basis (with dilation and translation) to epitomize the image. Although WT has demonstrated its efficiency in denoising, but for natural images, however, there is a rich volume of dissimilar native basic patterns, which cannot be well characterized by using only one fixed wavelet basis.

To overcome the problem of WT a spatially adaptive Principal Component Analysis (PCA) based denoising scheme is presented by Muresan and Parks [14], which computes the locally fitted basis to transform the image. Elad and Aharon [4,7] presented rare redundant representation and K-SVD based denoising algorithm by training a highly over-complete dictionary. Another denoising technique based on shape-adaptive Discrete Cosine Transform (DCT) to the neighborhood is presented by Foi et al. [3]. All these techniques lead to effective denoising and show better denoising performance than the conventional WT-based denoising algorithms.

Recently established non-local means (NLM) approaches [26]use a very different viewpoint from the above methods, where the similar image pixels are averaged according to their intensity distance. In [18], the NLM denoising background was well established. Each pixel is estimated as the weighted average of all the pixels in the image, and the weights are determined by the similarity between the pixels. This structure was enhanced in [19], where the pair wise hypothesis testing was used in the NLM estimation. Inspired by the achievement of NLM methods, recently Dabov et al. [23], proposed a collaborative image denoising scheme by patch matching and sparse 3D transform. They searched for similar blocks in the image by using block matching and grouped those blocks into a 3D cube. A sparse 3D transform was then applied to the cube and noise was suppressed by applying Wiener filtering in the transformed domain. The so called BM3D scheme accomplishes amazing denoising results yet its implementation is a little multifarious.

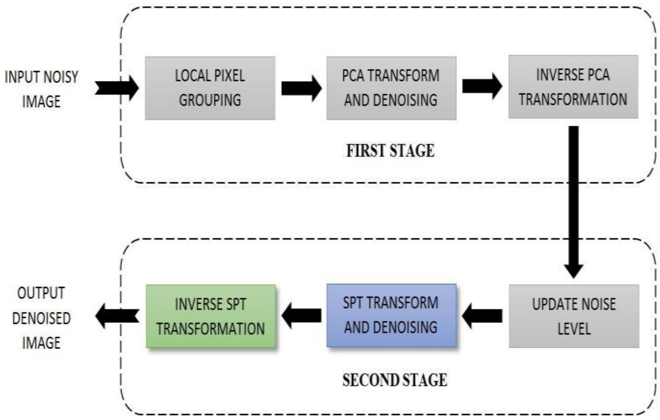

Fig.1. Flowchart of the proposed PCA-SPT denoising scheme

Recently a novel denoising scheme named LPG-PCA [24] is developed which can effectively preserve the image fine structures while smoothing noise. By transforming the original dataset into PCA domain and preserving only the several most significant principal components, the noise can be removed. In [15], a PCA-based scheme was suggested for image denoising by using a moving window to measure the local statistics, from which the local PCA transformation matrix was estimated.

In this paper we present an efficient LPG-PCA based denoising method with steerable pyramid transform (SPT). In the proposed PCA-SPT scheme, we model a pixel and its adjacent pixels as a vector variable. The training samples of this variable are selected by block matching scheme. With this LPG technique, the local statistics of the variables can be accurately calculated so that the image edge structures can be well protected after shrinkage in the PCA domain for noise removal. As shown in Figure 1, the proposed PCA-SPT algorithm has two stages. The first stage yields an initial estimation of the image by removing most of the noise content and the second stage will further refine the output of the first stage.

The first stage use the equivalent procedures as done in LPG-PCA denoising scheme, but in the second stage we use Steerable Pyramid Transform, to decompose images into frequency sub-bands. Before applying the second stage the level of noise is updated adaptively. The transform is implemented in the Fourier domain [10], allowing exact reconstruction of the image from the sub-bands. Since the noise is significantly reduced in the first stage, we do not use LPG in the second stage, which intern reduces the computational cost of the entire scheme. Compared with the BM3D algorithm, the proposed PCA-SPT technique can use a relatively small local window, like LPG-PCA algorithm to group the similar pixels for PCA training with reduced computational cost, yet it yields competitive results with state-of-the-art BM3D algorithm.

II. FIRST STAGE DENOISING PROCEDURE

It is clear that, denoising is a process to estimate and remove noise, from the corrupted images, Hence to create a denoising model, it is necessary to know about the noise type which contaminates the image. Here we assume that the noise which contaminates the original image is Additive White Gaussian Noise with zero mean μ and standard Deviation σ , i.e. $I_v = I + v$, where I_v is the noisy image. The original image I and v noise are presumed to be uncorrelated. The objective of denoising model is to find estimation, denoted by $\hat{I}$ of I from the observation I_v. The denoised image $\hat{I}$ is anticipated to be as close to I as possible.

The spatial location and intensity are the two parameters through which an image pixel may be described, while the local structure of the image represented as a set of neighboring pixels at different intensity levels. Since most of the important information of an image is expressed by its edge structures, hence edge preservation is most important in image denoising. To achieve the previously specified goal, in this paper we model a pixel and its nearest neighbors as a vector variable and execute noise reduction on the vector instead of the single pixel.

To model a vector variable we create a K × K window centered on the fundamental pixel to be denoised. It is denoted by $x = [x_1, x_2 \ldots x_m]^T$, $m = k^2$ the vector containing all the elements within the window.

Since the image considered here is noisy, hence it is denoted by

$$X_v = X + V \tag{1.1}$$

ISSN: 2278 – 7798

The noisy vector of X, where $X_v = [x_1^v, x_2^v, \ldots x_m^v]^T$, $\boldsymbol{v} = [v_1, v_2 \ldots . v_m]^T$ and $x_k^v = x_k + v_k$, $k = 1, \ldots, m$. to calculate X from X_v, we consider them as noiseless and noisy vector variables respectively, so that the statistical methods such as PCA may be used.

In order to eliminate the noise from X_v by using PCA transform, a set of training samples of X_v is required so that PCA transformation matrix can be calculated in terms of covariance matrix of X_v. To find the training samples, we create a training block of size L × L (L >K) centered on X_v, as demonstrated in Fig. 2. It is very easy to take the image pixel in each possible block of size K ×K within the training block of size L×L as the samples of noisy variable X_v.

In this way, there are totally $(L - K + 1)^2$ training samples for each component x_k^v of x_v. However, there may be very different blocks from the given central K × K block in the L × L training window so that taking all the K × K blocks as the training samples of x_v will lead to wrong approximation of the

covariance matrix of x_v. Inaccurate approximation of the PCA transformation matrix will occur due to faulty estimate of the training samples, which intern increases the noise residuals in the denoised image. Hence, it is very essential to select and group the training samples before employing the PCA for denoising, which is similar to the central K × K block.

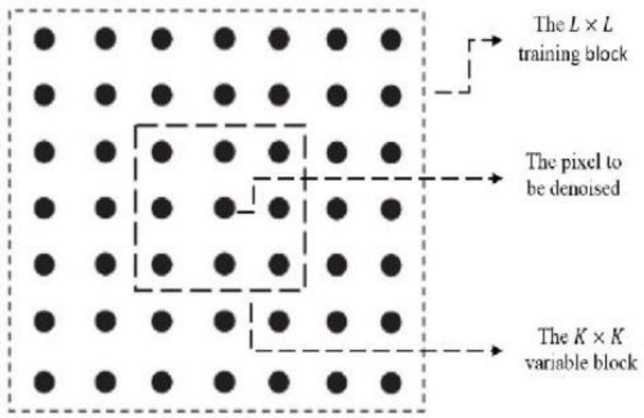

Fig. 2. Illustration of the modeling of first stage denoising.

covariance matrix of x_v. Inaccurate approximation of the PCA transformation matrix will occur due to faulty estimate of the training samples, which intern increases the noise residuals in the denoised image. Hence, it is very essential to select and group the training samples before employing the PCA for denoising, which is similar to the central K × K block.

Grouping of the training samples is same as to the central K × K block in the L × L training window. It is surely a classification scheme that may be realized by various techniques such as block matching, correlation-based matching, fuzzy clustering [27], K-means clustering [28], self-organizing maps [29] etc. and choice of this algorithm is based on different criteria. Among them, the block matching method is very simple and efficient. Hence we use block matching method for local pixel grouping procedure.

There are totally $(L \times K + 1)^2$ possible training blocks of x_v in the L × L training window. We used the fact that noise is AWGN and uncorrelated with signal. For computing the PCA transformation matrix it is necessary, that there should be adequate number of samples. To estimate the image local statistics optimized training samples are used. They are robust and make the algorithm more stable to estimate the PCA transformation matrix. The next step is how to calculate the noiseless dataset X from the noisy observation X_v. Once we get X the central block and the central pixel under test can be extracted. Now each pixel is processed by such scheme, to denoised the entire image .

III. SECOND STAGE DENOISING PROCEDURE

As discussed in the above section, LPG-PCA procedure will remove most of the noise present in the image under test. Still, the denoised image has as much noise residual, which makes the image visually unpleasant. Fig.3 shows an example of image Baby. Fig. 3(a) is the original image Baby; Figure 3(b) is the noisy version of it (σ =10 , PSNR=28.1dB); Figure 3(c) is the denoised image (PSNR= 35.1dB, SSIM = 0.9523) by using the basic LPG-PCA scheme. Although both the parameters PSNR and SSIM are much improved, still we can see much noise residual in the output denoising image. One of the basic reasons for the presence of noise residual in the denoised image is that the original dataset X_v is contaminated with strong noise, which makes the covariance matrix $\omega_{\bar{x}_v}$ noisier and leads to estimation bias of the PCA transformation matrix. This in turn degrades the performance of denoising procedure.

Original dataset contaminated with strong noise is another reason that leads to LPG errors, which accordingly leads to the estimation bias of the covariance matrix $\omega_{\bar{x}}$ (or $\omega_{\bar{x}_v}$). Thus, for a better noise reduction, it is necessary to remove noise residuals present after denoising. Since, most of the noise is removed by first stage LPG-PCA denoising procedure, which can improve the accuracy and the estimation of ($\omega_{\bar{x}}$ (or $\omega_{\bar{x}_v}$).of the denoised image. Now to increase the denoising results, it is important to use a denoising scheme one more time to denoised image. Although, the concept of two stage denoising is already established in [24], which uses the same algorithm in the refinement of second stage also. We use the same concept in this paper, in which we use LPG-PCA for the first stage of denoising and SPT for the second stage of denoising. SPT decomposes images into frequency sub-bands, here the noise residuals present after second stage is easily suppressed.

ISSN: 2278 – 7798

Fig. 3. (a) Original image Baby; (b) noisy image (PSNR= 28.1 dB) :(c) denoised image after the first stage of the proposed method (PSNR= 34.6 dB) and (d) denoised image after the second stage of the proposed method (PSNR=35.2 dB). We see that the visual quality is much improved after the second stage refinement.

Fig. 3(d) shows the denoising results (PSNR=35.2 dB) of Image Baby after the second denoising stage. Although the PSNR is improved by only 0.6 dB, but the visual quality of the image is much improved by effectively removing the noise residual in the second denoising stage.

IV. EXPERIMENTAL RESULT AND ANALYSIS

The concept of the proposed PCA-SPT algorithm is carried from the antecedently developed LPG-PCA denoising algorithm. The proposed PCA-SPT algorithm is a prolongation of the LPG-PCA denoising algorithm [24].We used 8 different images to enumerate the performance of the proposed algorithm. Our dataset includes standard test images . We will evaluate the data for Baby, Leopard, Cameraman, Flower, Man, Monarch, Duck and Ship shown in Fig.4. All of our images are 8-bit gray scale images of dimension 256 × 256 and are converted to same image format (i.e. TIF) using MATLAB.

The results presented in this paper are obtained by adding simulated AWGN to true noiseless images. After denoising the results are compared with the true noiseless image for performance evaluation. Due to the space limitation, we demonstrate the comparison result of proposed scheme with only some values of noise level. We analyzed the complete dataset of test images with noise levels i.e. σ= 10, 20, 30, 40. To represent the denoising performance of our algorithm, we compare the proposed scheme with four representative and state-of-the-art denoising algorithms: the wavelet-based denoising methods [3,6]; Po-Edges denoising methods[10]; LPG-PCA denoising method [24] and the recently developed BM3D denoising method[23]. The BM3D algorithm is state of- the-art denoising algorithm and it has been considered as a standard for developing novel denoising algorithm.

Fig. 4. The test images Baby, Leopard, Cameraman, Flower, Man, Monarch, Duck, and Ship.

PSNR and SSIM measures of previously established denoising scheme and the proposed method on the 8 test images are summarized in Table I. Let's first see the PSNR measures by different methods. From Table II we observe that the BM3D filtering method of denoising has the highest PSNR measures. The PSNR result of proposed method is higher than the wavelet [3,6], Po-Edges [10], LPG-PCA [24]and the wavelet-based method [3,6] has the lowest PSNR value. Let's then focus on the SSIM measure and the visual quality evaluation of these denoising algorithms. From Table II it is clear, that BM3D has the highest SSIM measures. The proposed PCA-SPT has higher SSIM measures than LPG-PCA [24]. Again, the wavelet-based denoising methods have the lowest SSIM measures.

Due to the limitation of space, in this paper we can only show partial denoising results. Fig. 5 and Fig. 7 show the denoising results of the two test images with noise level σ = 20 by different methods. The subfigure (a) is the original image; subfigures (b-f) are the denoised images by the scheme in [3,6], [10], [24],[23]and the proposed PCA-SPT method respectively. We see that although BM3D has higher SSIM measures than proposed PCA-SPT method, their denoised images are analogous in real visual observation, and they have much improved visual quality than all the other techniques. Graphical representation of PSNR measures for image Cameraman by different schemes are shown in Fig. 6and for image Monarch in Fig. 8 respectively. The graph shows that when the PSNR measure of the proposed scheme is almost equals to the other methods. The LPG-PCA scheme generates many artifacts in the denoised image.

ISSN: 2278 – 7798

Fig. 5. The denoising results of Cameraman by different schemes. (a) Noiseless Cameraman; denoised images by methods (b)[3,6]; (c) [10]; (d) [24]; (e) [23]; and (f) the proposed PCA-SPT method.

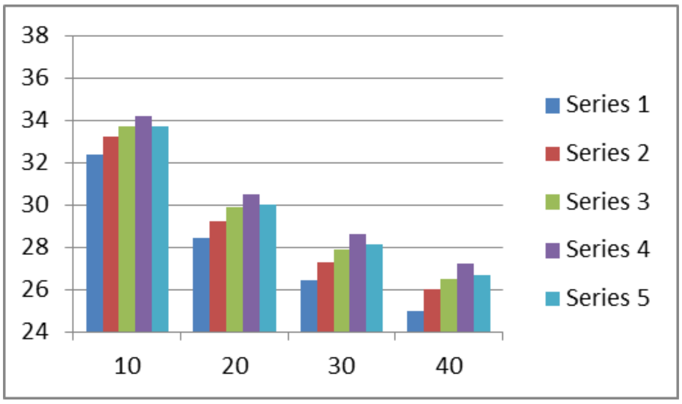

Fig. 6. Graphical representation of PSNR measure (in dB) for Image Cameraman by different schemes.

The wavelet based denoising methods [3,6]have the worst visual quality. This is because in WT, the fixed wavelet basis function is used to de-correlate the many different image structures. Often this is not efficient enough to represent the image content so that many denoising errors appear.

TABLE I

THE PSNR (DB) AND SSIM RESULTS OF THE DENOISED IMAGES AT DIFFERENT NOISE LEVELS AND BY DIFFERENT SCHEMES

Method	[1,2]	[3]	[40]	[45]	Proposed
Baby					
σ = 10	34.0(0.9050)	34.8(0.9202)	35.1(0.9523)	35.4(0.9588)	35.2(0.9518)
σ = 20	29.5(0.8054)	30.7(0.8505)	30.9(0.8909)	31.2(0.9124)	31.0(0.8937)
σ = 30	27.2(0.7302)	28.3(0.7865)	28.3(0.8215)	28.7(0.8651)	28.6(0.8350)
σ = 40	25.6(0.6757)	27.0(0.7503)	26.6(0.7509)	26.9(0.8906)	26.9(0.7972)
Leopard					
σ = 10	33.2(0.9193)	34.4(0.9378)	34.3(0.9360)	34.6(0.9449)	34.5(0.9393)
σ = 20	29.1(0.8330)	30.3(0.8636)	30.0(0.8509)	30.6(0.8794)	30.3(0.8660)
σ = 30	27.1(0.7635)	28.2(0.8034)	27.7(0.7687)	28.4(0.8209)	28.1(0.7999)
σ = 40	25.7(0.6977)	26.6(0.7366)	26.2(0.6955)	26.8(0.7646)	26.6(0.7407)
Cameraman					
σ = 10	32.4(0.8913)	33.2(0.9118)	33.7(0.9256)	34.2(0.9319)	33.7(0.9250)
σ = 20	28.4(0.8018)	29.3(0.8357)	29.9(0.8551)	30.5(0.8755)	30.0(0.8626)
σ = 30	26.4(0.7400)	27.3(0.7836)	27.9(0.7933)	28.6(0.8373)	28.1(0.8153)
σ = 40	25.1(0.6972)	26.0(0.7507)	26.5(0.7369)	27.2(0.8057)	26.7(0.7783)
Flower					
σ = 10	33.3(0.9083)	34.5(0.9306)	35.0(0.9399)	35.4(0.9483)	35.1(0.9424)
σ = 20	29.0(0.8074)	30.4(0.8609)	31.0(0.8696)	31.6(0.8971)	31.1(0.8789)
σ = 30	27.0(0.7371)	28.1(0.7968)	28.7(0.8014)	29.4(0.8496)	28.9(0.8257)
σ = 40	25.3(0.6712)	26.6(0.7431)	27.2(0.7397)	27.7(0.8022)	27.4(0.7766)
Man					
σ = 10	33.1(0.8872)	34.0(0.9075)	34.0(0.9370)	34.3(0.9391)	34.1(0.9316)
σ = 20	29.3(0.7702)	30.1(0.8059)	30.2(0.8503)	30.5(0.8634)	30.3(0.8428)
σ = 30	27.5(0.6959)	28.3(0.7327)	28.2(0.7661)	28.7(0.8030)	28.4(0.7769)
σ = 40	24.4(0.6303)	27.1(0.6695)	27.0(0.6898)	27.6(0.7530)	27.3(0.7113)
Monarch					
σ = 10	32.1(0.9216)	33.4(0.9419)	34.0(0.9530)	34.1(0.9557)	34.1(0.9546)
σ = 20	28.0(0.8521)	29.4(0.8911)	30.0(0.9053)	30.4(0.9179)	30.2(0.9143)
σ = 30	25.8(0.7869)	27.2(0.8480)	27.7(0.8539)	28.4(0.8821)	27.8(0.8692)
σ = 40	24.4(0.7447)	25.6(0.8067)	26.1(0.8029)	26.7(0.8446)	26.5(0.8365)
Duck					
σ = 10	35.0(0.9326)	35.8(0.9475)	36.0(0.9484)	36.4(0.9567)	36.3(0.9542)
σ = 20	31.0(0.8700)	32.0(0.9018)	28.4(0.8913)	32.6(0.9181)	32. 4(0.9130)
σ = 30	29.0(0.8270)	30.0(0.8692)	30.0(0.8346)	30.6(0.8839)	30.2(0.8684)
σ = 40	27.6(0.7903)	28.6(0.8399)	28.5(0.7802)	29.1(0.8542)	28.8(0.8397)

ISSN: 2278 – 7798

Ship					
σ = 10	31.8(0.9290)	32.7(0.9447)	32.6(0.9434)	32.9(0.9494)	32.8(0.9472)
σ = 20	27.5(0.8551)	28.6(0.8849)	28.4(0.7842)	28.7(0.8906)	28.6(0.8879)
σ = 30	25.4(0.7922)	26.4(0.8325)	26.2(0.8042)	26.5(0.8358)	26.4(0.8269)
σ = 40	24.0(0.7332)	24.9(0.7716)	24.7(0.7362)	25.0(0.7825)	25.0(0.7771)

The proposed PCA-SPT denoising procedure uses PCA to adaptively compute the local image decomposition transform so that it can better represent the image local structure. In addition, the SPT operation is employed to eliminate the noise residuals present after first stage denoising, that decompose images into frequency sub-bands. Before applying the second stage the level of noise is update adaptively. The transform is implemented in the Fourier domain, allowing exact reconstruction of the image from the sub-bands. The denoised images by BM3D and the proposed scheme are very comparable in terms of visual quality. Both of them can well preserve the image edges and remove the noise without introducing too many artifacts. Although the PSNR and SSIM measure of PCA-SPT are lower than that of BM3D,

PCA-SPT has competitive results in the preservation of small edge structure as the original LPG-PCA method.

In summary, as a non-local collaborative denoising scheme, BM3D can successfully exploit the non-local redundancy in the image to suppress noise. Therefore, it could have very high PSNR and SSIM measures. However, for fine-grain structures, improper non-local information may be introduced by BM3D for image restoration so that errors may be produced in those areas. Although the LPG-PCA scheme works well for fine-grain preservation but its computational cost is high than PCA-SPT since it uses block matching in both stages. The computational cost of PCA-SPT is very low than LPG-PCA algorithm, hence PCA-SPT works well in small structure preservation with low computational cost.

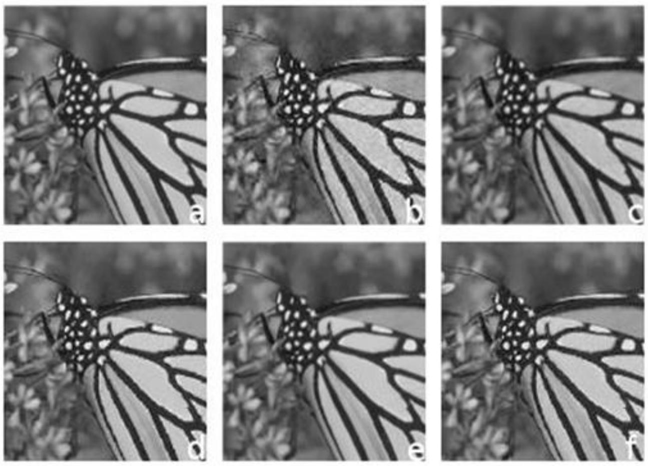

Fig. 7. The denoising results of Monarch by different schemes. (a) Noiseless Monarch; denoised images by methods (b)[3,6]; (c) [10]; (d) [24]; (e) [23]; and (f) the proposed PCA-SPT method.

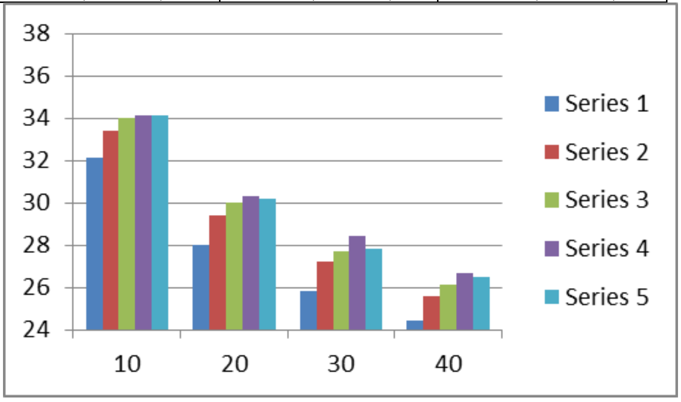

Fig. 8. Graphical representation of PSNR measure (in dB) for Image Monarch by different schemes.

V.CONCLUSION

The proposed PCA-SPT denoising method employs PCA transform with LPG in first stage. Principal component analysis adaptively calculate the vector decomposition of the target image, hence it can better represent the local structure of image and local pixel grouping, which ensure that only the right samples of pixels are needed in the training of PCA transform. In addition to PCA with LPG operation we incorporate the second stage, in which SPT is used. Computational cost of the second stage is approximately one fourth of the first stage of LPG-PCA algorithm. Thus the overall cost of the proposed algorithm is very low and we get the denoising result in less time than that required in LPG-PCA algorithm. It provides a good compromise between the accuracy and the execution time: it is much faster and considerably more accurate than the LPG-PCA algorithm.

REFERENCES

[1] Scott E. Umbaugh, *Digital image processing and analysis:human and computer vision applications with CVIPtools*.: CRC press, 2010.

[2] Rafael C. Gonzalez, Richard E. Woods, and Steven L. Eddins, *Digital Image Processing* , 2nd ed. Englewood Cliffs, NJ: Prentice- Hall, 2002.

[3] D. L. Donoho, "Denoising by soft thresholding," *IEEE Transactions on Information Theory*, pp. 613–627, 1995.

[4] R. R. Coifman and D. L. Donoho, *Translation-invariant de-noising*, G. Oppenheim, Ed. Berlin, Germany: Springer, 1995.

[5] M. K. Mıhcak, I. Kozintsev, K. Ramchandran, and Moulin P., "Low-complexity image denoising based on statistical modeling of wavelet coefficient," *IEEE Signal Processing Letters*, vol. VI, no. 12, pp. 300–303, 1999.

[6] S. G. Chang, B. Yu, and M. Vetterli, "Spatially adaptive wavelet thresholding with context modeling for image denoising," *IEEE Transaction on Image Processing*, vol. IX, no. 9, pp. 1522–1531, 2000.

[7] A. Pizurica, W. Philips, I. Lamachieu, and M. Acheroy,

ISSN: 2278 – 7798

"A joint inter- and intrascale statistical model fo Bayesian wavelet based image denoising," *IEEE Transaction on Image Processing* , vol. V, no. 11, pp. 545–557, 2002.

[8] L Zhang, B Paul, and X Wu, "Hybrid inter- and intra wavelet scale image restoration," *Pattern Recognition*, vol. VIII, no. 36, pp. 1737–1746, 2003.

[9] Z Hou, "Adaptive singular value decomposition in wavelet domain for image denoising," *Pattern Recognition*, vol. VIII, no. 36, pp. 1747–1763, 2003.

[10] J. Portilla, V. Strela, M. J. Wainwright, and E. P. Simoncelli, "Image denoising using scale mixtures of Gaussians in thewavelet domain," *IEEE Transaction on Image Processing* , vol. XI, no. 12, pp. 1338–1351, 2003.

[11] P. Bao, X. Wu L. Zhang, "Multiscale LMMSE-based image denoising with optimalwavelet selection," *IEEE Transaction on Circuits and Systems for VideoTechnology*, vol. IV, no. 15, pp. 469–481, 2005.

[12] A. Pizurica and W. Philips, "Estimating the probability of the presence of a signal of interest in multiresolution single and multiband image denoising," *IEEE Transaction on Image Processing*, vol. III, no. 15, pp. 654–665, 2006.

[13] J. L. Starck, E. J. Candes, and D. L. Donoho, "The curvelet transform for image denoising," *IEEE Transaction on Image Processing*, vol. VI, no. 11, pp. 670–684, 2002.

[14] G. Y. Chen and B. Kegl, "Image denoising with complex ridgelets," *Pattern Recognition*, vol. II, no. 20, pp. 578–585, 2007.

[15] D. D. Muresan and T. W. Parks, "Adaptive principal components and image denoising," in *Proceedings of the 2003 International Conference on Image Processing*, vol. 1, 14–17 September 2003, pp. 101–104.

[16] C. Tomasi and R. Manduchi, "Bilateral filtering for gray and colour images," in *IEEE International Conference on Computer Vision*, Bombay, India, 1998, pp. 839–846.

[17] D. Barash, "A fundamental relationship between bilateral filtering, adaptive smoothing, and the nonlinear diffusion equation," *IEEE Transaction on Pattern Analysis and Machine Intelligence*, vol. VI, no. 24, pp. 844–847, 2002.

[18] A. Buades, B. Coll, and J. M. Morel, "A review of image denoising algorithms, with a new one," *Multiscale Modeling Simulation*, vol. II, no. 4, pp. 490–530, 2005.

[19] C. Kervrann and J. Boulanger, "Optimal spatial adaptation for patch based image denoising," *IEEE Transaction on Image Processing*, vol. X, no. 15, pp. 2866–2878, 2006.

[20] M. Elad and M. Aharon, "Image denoising via sparse and redundant representations over learned dictionaries," *IEEE Transaction on Image Processing*, vol. XII, no. 15, pp. 3736–3745, 2006.

[21] M Aharon, M Elad, and A M Bruckstein, "The K-SVD: an algorithm for designing of overcomplete dictionaries for sparse representation," *IEEE Transaction on Signal Processing*, vol. XI, no. 54, pp. 4311–4322, 2006.

[22] A. Foi, V. Katkovnik, and K. Egiazarian, "Pointwise shape-adaptive DCT for high quality denoising and deblocking of grayscale and color images," *IEEE Transaction on Image Processing*, vol. V, no. 16, 2007.

[23] K. Dabov, A. Foi, V. Katkovnik, and Egiazarian K., "Image denoising by sparse 3D transform-domain collaborative filtering," *IEEE Transaction on Image Processing*, vol. VIII, no. 16, pp. 2080–2095, 2007.

[24] L. Zhang, W. Dong, D. Zhang, and G. Shi, "Two-stage image denoising by principal component analysis with local pixel grouping," *Pattern Recognition*, vol. IV, no. 43, pp. 1531-1549, 2010.

[25] S. Mallat, *A Wavelet Tour of Signal Processing*. New York: Academic Press, 1998.

[26] L. P. Yaroslavsky, *Digital Signal Processing—An Introduction*. Berlin: Springer, 1985.

[27] F. Höppner, F. Klawonn, R. Kruse, and t Runkler, *Fuzzy Cluster Analysis*. Chichester: Wiley, 1999.

[28] J. B. MacQueen, "Some methods for classification and analysis of multivariate observations," in *Berkeley Symposium on Mathematical Statistics and Probability*, Berkeley, 1967, pp. 281–297.

[29] T. Kohonen, *Self-Organizing Maps*, 2nd ed. Heidelberg: Information Sciences Springer, 1997.

[30] E. P. Simoncelli, W. T. Freeman, E. H. Adelson, and D. J. Heeger, "Shiftable multi-scale transforms," *IEEE Transaction on Information Theory*, vol. 38, pp. 587–607, Mar 1992.

[31] W. T. Freeman and E. H. Adelson, "The design and use of steerable filters," *IEEE Pattern Anal. Machine Intell.*, vol. 13, no. 9, pp. 891–906, 1991.

[32] Z. Wang, A.C. Bovik, H.R. Sheikh, and E.P. Simoncelli, "Image quality assessment: from error visibility to structural similarity," *IEEE Transaction on Image Processing* , vol. 13, no. 4, 2004.

ISSN: 2278 – 7798